A novel CCD design for curvature wavefront sensing

Reinhold J. Dorn*[a], James W. Beletic[b] and Barry E. Burke[c]

[a]European Southern Observatory, Karl Schwarzschildstr. 2, D-85748 Garching, Germany
[b]Rockwell Scientific, 5212 Verdugo Way,Camarillo, CA 93012, USA
[c]MIT Lincoln Laboratory, 244 Wood Street, Lexington, MA 02420-9108, USA

ABSTRACT

At the European Southern Observatory (ESO) in Garching, Germany, several adaptive optics systems using curvature wavefront sensors are being developed for the Very Large Telescope (VLT) and the VLT interferometer (VLTI). Curvature AO-systems have traditionally used avalanche photodiodes (APDs) as detectors due to strict requirements of very short integration times (200 microsec) and very low readout noise. Advances in CCD technology motivated an investigation of the use of a specially designed CCD as the wavefront sensor detector in a 60-element curvature AO system. A CCD has never been used before as the wavefront sensor in a low light level curvature adaptive optics system. This CCD can achieve nearly the same performance as APDs at a fraction of the cost and with reduced complexity for high order wavefront correction. Moreover the CCD has higher quantum efficiency and a greater dynamic range than APDs. A readout noise of less than 1.5 electrons at 4000 frames per second was achieved. Back-illuminated thinned versions of this CCD can replace APDs as a new detector for high order curvature wavefront sensing.

Keywords: CCD, APD, curvature sensing, adaptive optics, detectors

1. INTRODUCTION

Curvature AO-systems have traditionally used avalanche photo diodes (APDs) as detectors. APDs are photon-counting devices that produce a pulse on their output whenever a photon is detected. APDs have no read-out noise and read-out is almost instantaneous. However, they have some serious drawbacks compared to charge-coupled devices (CCDs):

- ***Small dynamic range*:** For the duration of the avalanche of electrons ñ typically around 40 ns ñ the APD is blind to any new photons arriving. This limits the dynamic range of the APD and requires the use of neutral density filters to adapt the incident photon flux to the dynamic range of the APD. CCDs, on the other hand, have an enormous dynamic range and thus require no filters.
- ***Low quantum efficiency*:** The quantum efficiency, which is the probability that an incident photon is detected, is lower for APDs than for CCDs. APDs typically have a peak quantum efficiency of 70% at 700nm, while the same number for CCDs is over 90%.
- ***High dark current*:** APDs generate dark current, or false photon counts, of 100 to 250 counts per second depending on the cost of the APDs, while a well-cooled CCD generates a negligible amount of dark current. The dark current affects the performance of the system when faint guide stars are used.
- ***High cost:*** A 60-element AO-system using APDs is significantly more expensive than one using a CCD.

The above facts combined with advances in CCD-technology motivated an investigation of the use of a special-purpose curvature-CCD as the wavefront sensor detector in a 60-element curvature AO system [2,3]

* reinhold.dorn@eso.org; phone +49-89-32006547; fax +49-89-3202362; www.eso.org

2. CURVATURE SENSING - HOW DOES IT WORK?

Curvature wavefront sensors are used in two of the most successful astronomical AO systems [1]. A curvature measures the intensity I_1 in an intrafocal plane and the intensity I_2 in an extrafocal plane and compares these intensities to determine the curvature of the wavefront. The normalised difference, $(I_1 - I_2)/(I_1+I_2)$, is used to reconstruct the wavefront. An oscillating membrane mirror is used to modulate the location of the plane being imaged on a single detector. During one half-cycle of the membrane motion, the detector records the intrafocal distribution of light, and during the other half-cycle it records the extrafocal distribution. In principal, only one out of focus image is needed to measure the wavefront curvature. However, using both the intrafocal and extrafocal images makes a curvature system work better for several reasons: (a) there is automatic compensation of systematic errors - variation in quantum efficiency, electronic gain, etc., (b) there is compensation of atmospheric scintillation, and (c) the control signal is simple ñ move the deformable mirror so that the intensity difference is zero. In a curvature AO system, the goal is to make the intensities equal on both sides of focus ñ this will occur when the wavefront is flat.

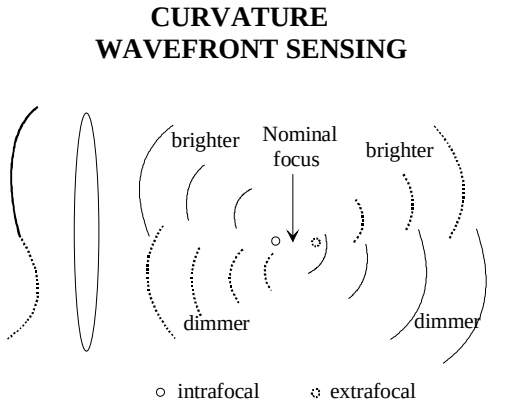

Figure 1 A schematic diagram of the principles of curvature wavefront sensing.

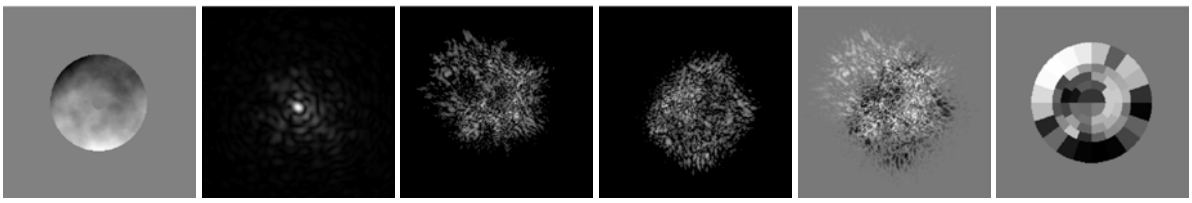

Figure 2 Computer simulation of curvature wavefront sensing.: (a) wavefront distortion, (b) infrared focal plane image, (c) intrafocal image, (d) extrafocal image (e) curvature signal at high resolution, (f) curvature signal binned into 60 subapertures. Simulation parameters: 0.66 arcsec seeing (at 500 nm), sensing wavelength = 700 nm (monochromatic), infrared image wavelength = 2.2 µm, out of focus distance = 25 cm, telescope focal length = 400 m, telescope diameter = 8 m with 14% obscuration from 1.12 m diameter secondary. Photon noise has not been simulated ñ all signals are ì infiniteî light level.

A more realistic curvature signal is shown in Figure 2, which presents a Kolmogorov atmospheric wavefront distortion, the infrared focal plane image, intrafocal and extrafocal images and the curvature signal. These signals were generated using a computer simulation [4]. In Figure 2, the AO loop is not running and thus the curvature

signal extends well beyond the pupil. The speckle structure of the out of focus images is partially due to monochromatic light assumed in the simulation and integration over the 400-1000 nm bandpass of a silicon sensor would have a smoother structure. Picture (f) shows the signal binned into 60 subapertures. Practically this is done via a lenslet array

3. ARCHITECTURE OF THE CURVATURE CCD

CCDs have not traditionally been used for curvature wavefront sensing since a standard geometry CCD with readout noise will give performance that is much worse than the performance of APDs. The key to making a CCD work in this application was on-chip integration. In order to fulfill the requirements, we utilized the following design options:

- Use of superpixels, i.e. bin on-chip, to loosen alignment tolerances.
- Layout pixels on a grid to lower risk, using fibers to feed from the lenslet array to the CCD, as is done with APD modules.
- Use multiple readout ports to have slower readout rates and hence lower readout noise.

This CCD has the ability to shift intrafocal and extrafocal photoelectrons integrated in a superpixel into charge storage areas on either side of the superpixel. The CCD can then be read out relatively slowly while the next integration starts on the chip. The architecture started with the definition of a unit cell (one subaperature).

3.1 Layout of one unit cell

Figure 3 shows a functional drawing of a unit cell, with an integration area made of 20 x 20 pixels, each 18 µm square. These form an imaging area (IA) of 360 by 360 µm for each subaperture, large enough to focus the light without optical crosstalk to other pixels. These pixels will be binned by rows into the storage areas SA and SB. The storage areas are small compared to the imaging area, being only one pixel wide.

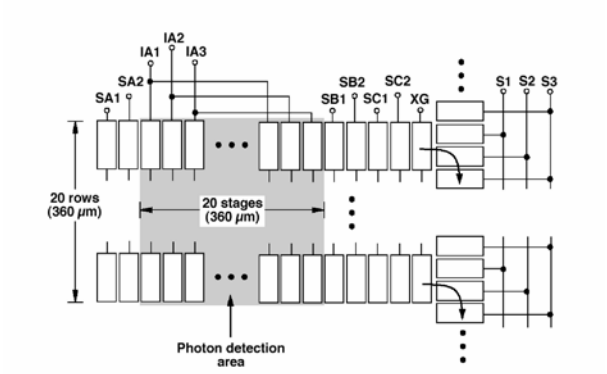

Figure 3 Unit cell overview - Superpixel architecture.

The SA and SB storage areas are used as a memory to store charge from the imaging area for multiple cycles of the membrane. After integration is completed the charge is moved into SC and then into the serial register for readout. The complete imaging area can be shifted into a storage area within 10 µsec, during the relatively flat portion of the membrane oscillation. A minimum number of clock phases is used to move and store the charges in the storage areas. Storage SA and SB have only 2 phases to store and move the charge. Three phases are needed for the storage area SC (SC1, SC2, XG), since a transfer gate is required as a barrier between SC and the serial register

3.2 Layout of one unit column with associated readout amplifier

Ten unit cells in the vertical direction are combined to form one unit column. There are only 3 prescan pixels in the serial register (see Figure 4). Since each unit column is a collection of 10 unit cells and only 8 of the unit cells are needed, we have the possibility to leave the first 2 cells empty to ì warm upî the electronics for the 8 cells with light.

If there is no need to warm up the electronics, the spots are put close to the output amplifier and hence the warmup time is saved. In addition the two extra cells will gave flexibility to avoid cells with traps.

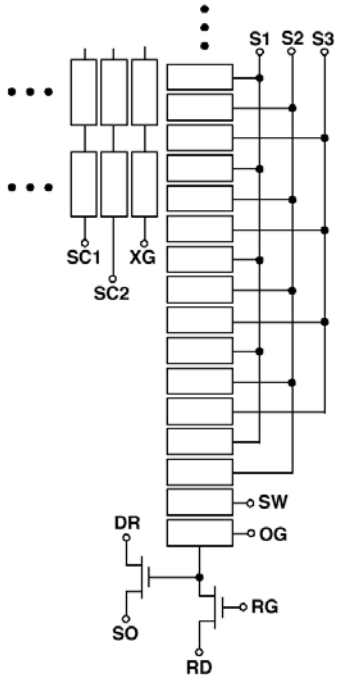

Figure 4 Unit column design - Schematic diagram with the clock phases and output amplifier circuit.

Figure 4 shows a schematic drawing of the unit column with the clock phases needed before the output amplifier circuit and also the phases needed for the output structure.

3.3 Tip/tilt sensor

Simulations showed that for a 60-element curvature system Strehl is improved with separate tip/tilt sensing. The CCID-35 also includes a tracker chip to be used as a tip/tilt sensor. The tracker chip simply integrates charge and reads out; there was no need for storage area SA, SB and SC. The tip/tilt sensor only has clocks IA1, IA2 and IA3 and XG. The tracker is a bit wider (24 pixels) since we expect to get at least 50 photoelectrons into each ìcellî of the tracker chip; the extra rows provide tolerance for alignment and the use of larger fibers. Since we only need 4 subapertures in the tracker, it has a reduced length of 160 pixels.

The tip/tilt sensor is clocked completely independently of the curvature WFS CCD portion of the device. One can integrate and read out this tip/tilt array at a different rate, although for noise reasons it might be useful to synchronize the clocks of both arrays.

3.4 Layout of the complete curvature CCD

To summarize the design, each superpixel consists of 20 x 20 pixels, where a pixel is 18 x 18 microns in size. The total height of each column is 10 superpixels or 200 pixels. There are 8 columns for a total of 80 superpixels and an independent tip/tilt sensor array. Figure 5 shows the CCD design of the curvature wavefront sensor array and Figure 6 pictures of the CCD. The total width of each unit column, including the gap, is 550 μm. There are substrate ground connections between the output circuit and the bottom of the imaging pixels to ensure good isolation of the clock waveforms from the output circuit. The output gates from the 8 outputs of the curvature array are connected together on the chip to minimize the pin count and simplify packaging. All of the corresponding clocks and bias lines for all unit columns are wired together on chip. Also the corresponding drive voltages for the amplifiers circuits are wired together. Only the drain voltages for the output amplifier are brought out separately to be able to optimize noise and linearity for each amplifier individually.

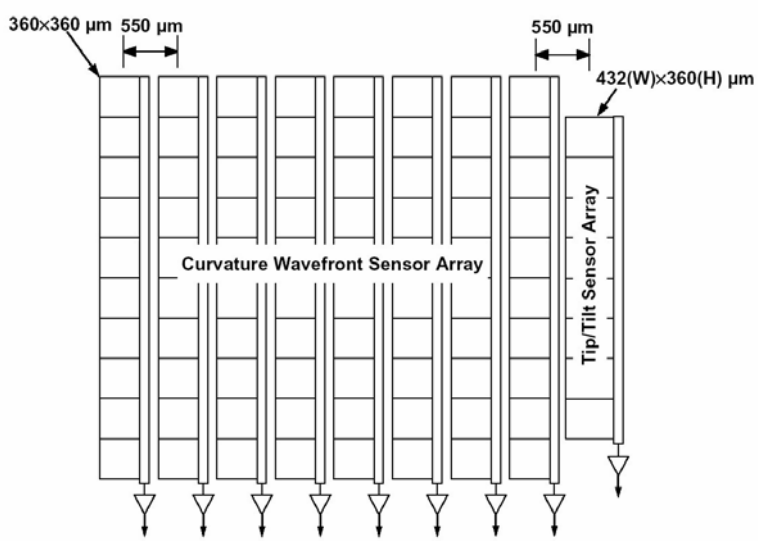

Figure 5 CCD design - curvature wavefront sensor array. The design consists of 80 unit cells. Ten unit cells are combined into a unit column. Each of these unit columns has an amplifier at the ì bottomî end of the serial register. On the right side of the device is the tip/tilt sensor.

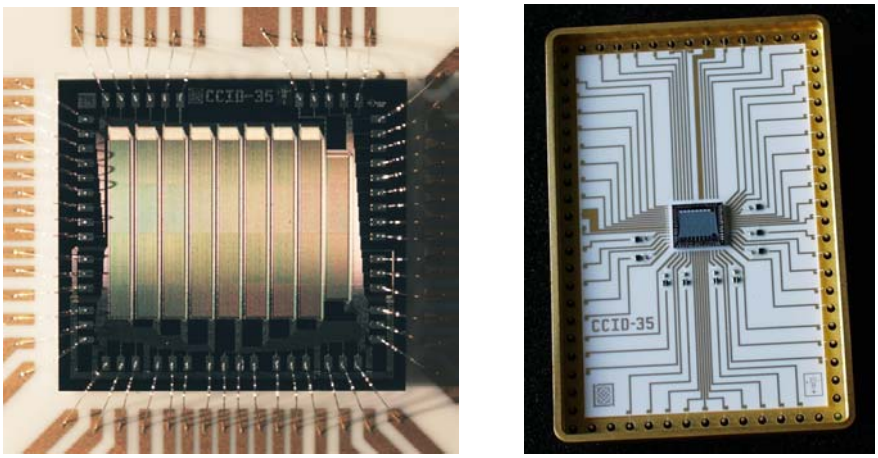

Figure 6 Pictures of the frontside device

3.5 Functionality and Readout modes

To illustrate the functionality of the curvature CCD, the following four examples of readout modes are shown. Figure 7a shows a dark frame of the curvature CCD in the non binned mode. Per readout port 200 image + 10 overscan pixels (including 3 prescan and 1 pipeline) are read out in the serial register and 20 image + 4 overscan pixels are read for the parallel lines. Figure 7b shows the same image but with the 60 spots of the fiberfeed projected via the Offner relay optics onto the CCD. Figure 7c shows an unbinned image with the charge for 10 extrafocal times stored in the storage pixels SA and the charge for 10 intrafocal times stored in the storage pixels SB. The light flux was kept constant during those exposures and hence the same amount of charge was stored in SA and SB. Finally Figure 7d shows the CCD in curvature mode, i.e. the pixels were binned 20 x 20 with the charge for 10 extrafocal times stored in the storage pixels SA and the charge for 10 intrafocal times stored in the storage pixels SB and then read out. For better visualization the parallels lines are overscanned by two superpixels.

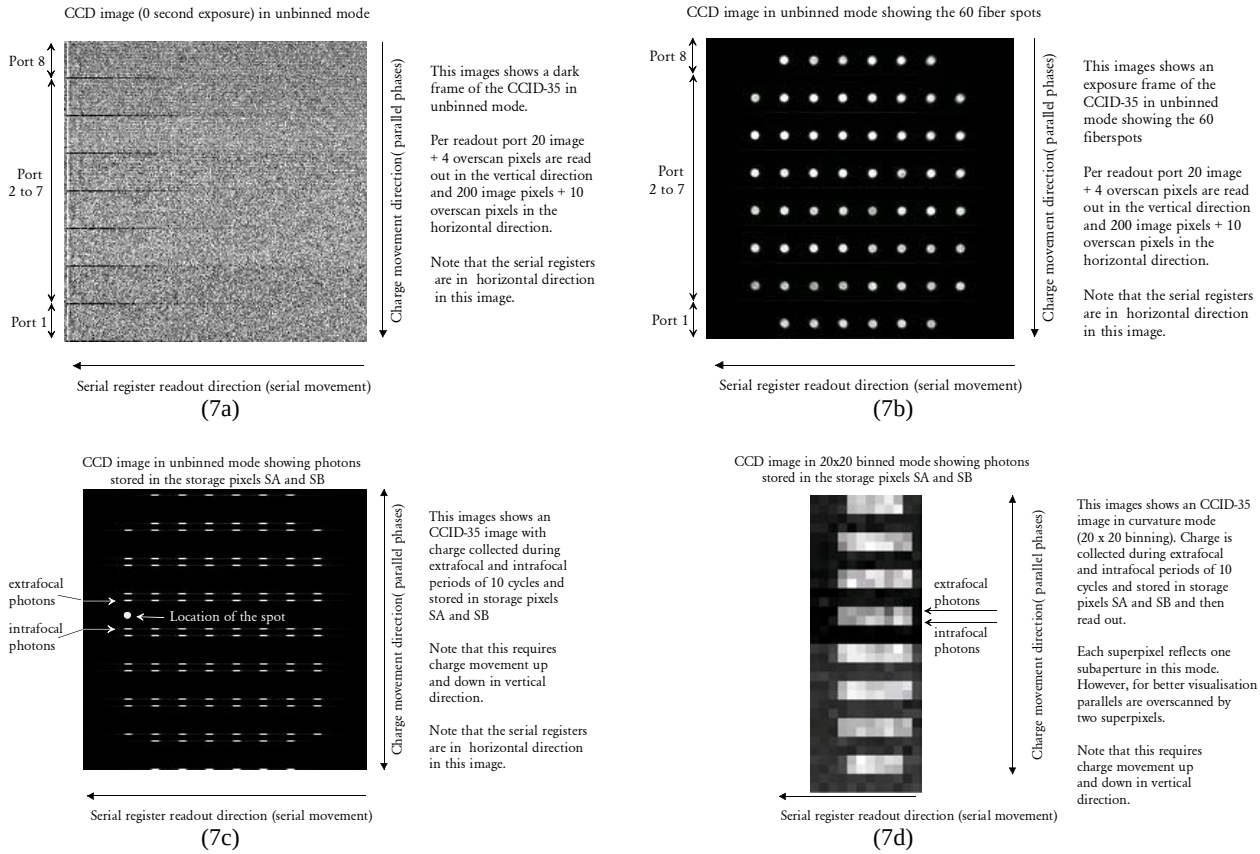

Figure 7 Functionality of the curvature CCD

4. PROTOTYPE SYSTEM AND CCD PERFORMANCE

To test the performance and the functionality of the curvature CCD, a laboratory system has been built to allow independent testing without the need to interface to a full adaptive optics system. An integrating sphere and a stable light source were used to simulate the membrane movement and providing the light signal for CCD characterization. An Offner relay optics was designed (consisting of two spherical, reflecting surfaces) to re-image the light of the fibers 1:1 onto the superpixels) and a fiberfeed with 60 individual fibers plus 4 additional fibers for the tip/tilt sensor to feed the subapertures of the CCD with light. A picture is shown in Figure 8.

At low light levels, for 14th magnitude and fainter stars, 1 to 2 electrons noise at a readout speed of 50,000 pixels/port/sec is required. A readout noise of less than 1.5 electrons was achieved for all readout ports including the tip/tilt sensor at a readout speed of 4000 frames per second. With all pixels per readout port binned into 12 superpixels, it was possible to read the serial register relatively slowly at 50 kilopixels per second with a measured responsivity of the CCID-35 of 14.2 µV/electron ± 5%. Figure 9 shows a typical readout noise and conversion factor versus drainvoltage. Vertical and horizontal CTE were measured better than 0.99999 down to lowest light levels with a residual non-linearity of the complete system better than 0.5% / -0.5%. (peak to peak). The CCD has a negligible amount of dark current at 197 Kelvin (0.25 electrons per subaperture at 50 Hz frame rate). The devices tested so far have excellent cosmetic quality which is highly important for a wavefront sensor and will be discussed in the next section in more detail.

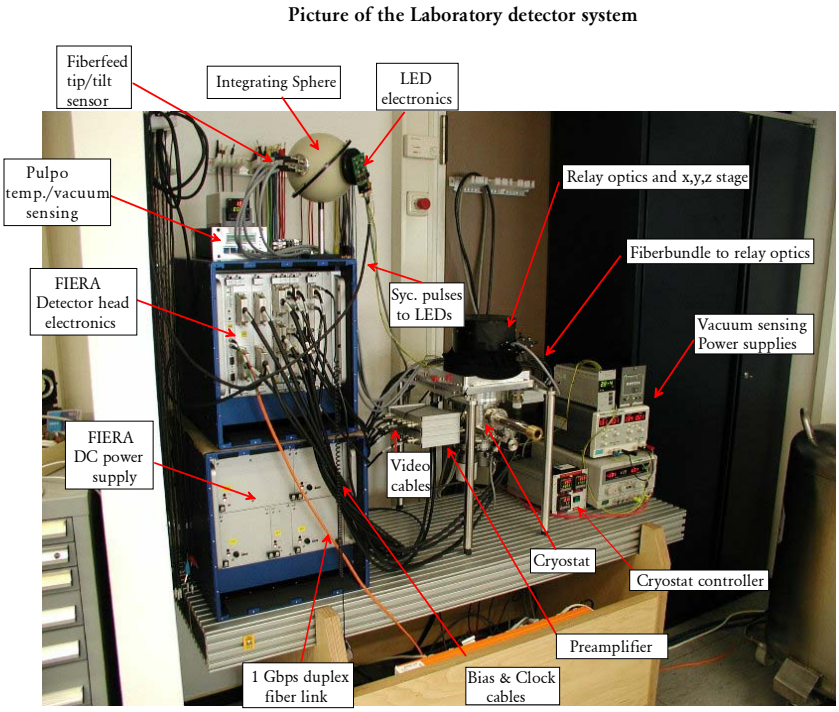

Figure 8 Picture of the prototype system

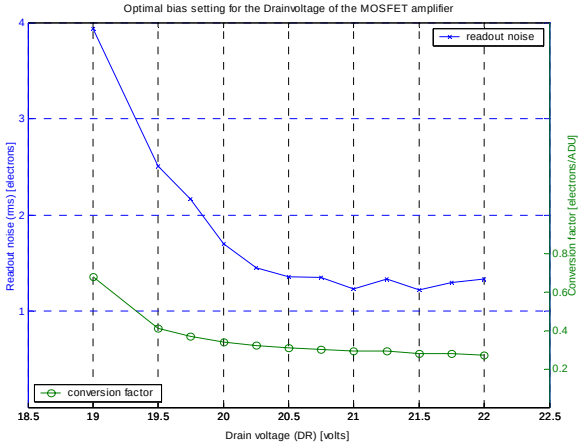

Figure 9 Readout noise and conversion factor versus drainvoltage

5. LOW LIGHT LEVEL OPERATION

Apart from the low noise capability of the curvature CCD, the CCD must also be able to transfer small charge packages down to one electron with high efficiency to be used as a low light level wavefront sensor in adaptive optics. Traps, which absorb and release electrons on a very short timescale can cause a fluctuation in the charge of the pixel and hence add to the noise of the CCD. CTE usually is dependent on the amount of charge being transferred because low-level cosmetic defects can trap small charge packages in a pixel. At low light levels

problems usually occur when the potential wells are almost empty or just have a small charge package stored. To be able to move single electrons with good charge transfer efficiency, there is a notch in the channel design of the CCID-35s, which reduces the ability of traps to capture electrons. This notch or trough is 2 microns wide in the image pixels and 3 microns wide in the serial pixels.

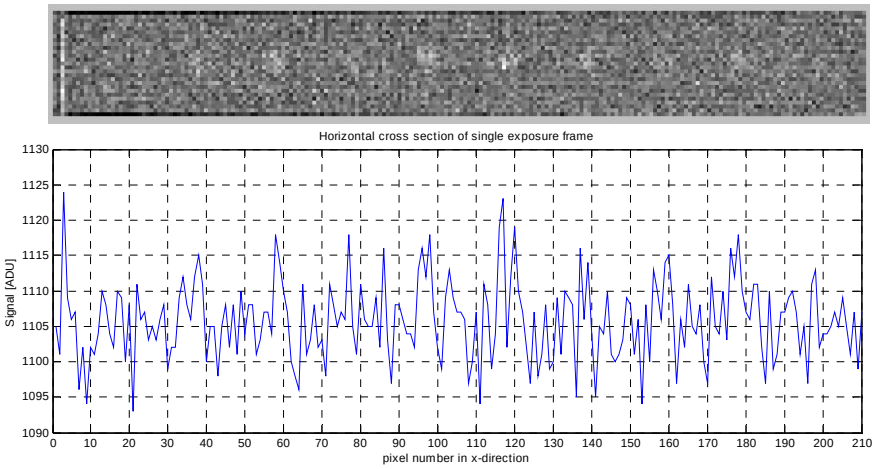

Figure 10 CCD image with ~ 1 electron charge per pixel and a readout noise of 1.4 electrons and its horizontal cross section.

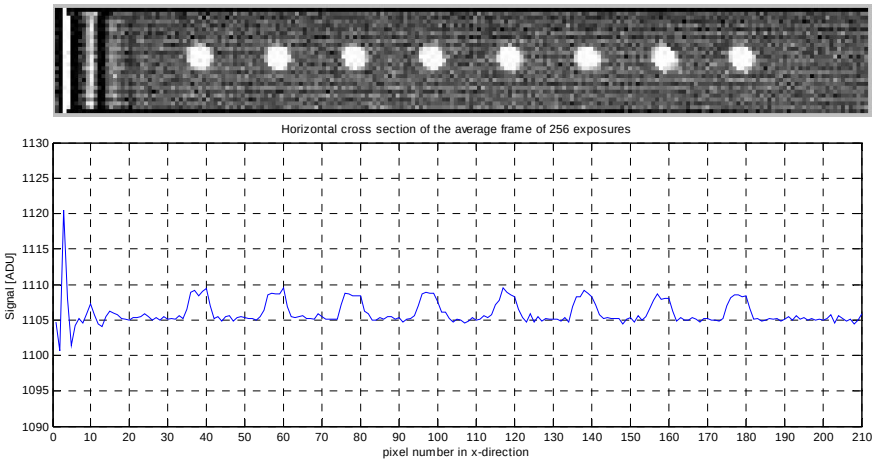

Figure 11 Average frame of 256 CCD image with ~1 electron charge per pixel and a readout noise of ~0.1 electrons and its horizontal cross section.

To verify the capability of the CCID-35s to move very small charge packets with high efficiency, the input illumination on the fiber entrance was turned down with neutral density filters to give a signal of ~1 electron per pixel per exposure. Figure 10 shows a strip of a CCD image for one amplifier with a readout noise of 1.4 electrons. The signal produced in the fiber spots is almost not visible and embedded in the noisy trace of the readout noise. Hence 256 exposures with the same illumination level were summed up and normalized. Figure 11 shows this image and the horizontal cross section of the spot signals.The charge is clearly visible and was measured to be 4 to 5 ADU (1 to 1.5 electrons) on average per pixel per frame. Due to averaging the single exposures, the signal to noise ratio was improved and the random noise was reduced and measured to be about 0.1 electrons.

Traps or blemishes however would also be seen in that image but the CCD has an extremely good cosmetic quality. The single electron events that made up the signal in the low light level frame are clearly separated in the average frame and indicate that single electrons have been transferred with a high efficiency throughout the device. The ramp-up effect seen at the beginning of the image (first 20 pixels) is not due to a trap in the CCD, it is due to a

warm-up effect in the electronics at the beginning of the readout of the serial register. Since the CCD consists of 80 subapertures there was no need to use the first superpixel of each CCD column.

Going to even lower light levels was one of the most interesting tests with the curvature CCD to show that the CCD can transfer also very low signal charges per subaperture i.e. a 20x20 binned superpixel. To verify this capability a single image taken at a specific light level was compared with another image obtained by adding a large number of individual images each taken at a much lower light level. Hence the total number of photons per pixel in the two images should be the same. This was done at a number of light levels and the results are very consistent. Figure 12 shows a series of images of the curvature CCD with the first 4 amplifiers of the CCD i.e. 30 subapertures. The first image is an exposure adding up charge for 4 cycles, resulting in an image with ~1 electron charge per subaperture. The signal is completely embedded in the noise of the frame. The second image shows the sum of 16 four-cycle images and the third image shows a sum of 256 four-cycle images added together. For both the 16 image sum and the 256 sum the signal in the individual subapertures is clearly visible. For comparison the last image shows a frame at much higher signal levels to identify the subapertures fed with photons by the fibers.

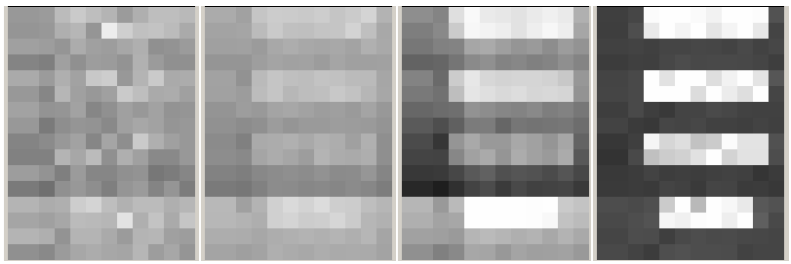

Figure 12 Images of one 4 cycle(1)exposure , 16 four cycle(2) exposures , 256 four cycle(3) exposures with ~1 electron charge per subaperture per 4 cycle image and one image at a higher signal level (4)

Figure 13 shows similar images of the same kind, but the LED has been switched on only during the intrafocal integration times of the readout mode. Hence only the subaperatures for the intrafocal photons contain the charge. This result also demonstrates that the CCD is not only able to move very low charge packages within the CCD, it shows also that the charge movement goes in the desired direction.

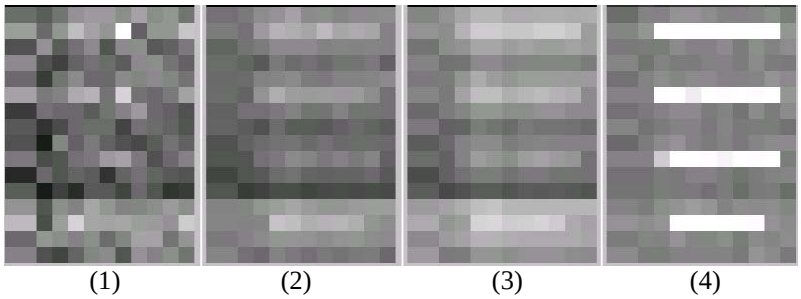

Figure 13 Images of one 4 cycle(1)exposure , 16 four cycle(2) exposures , 256 four cycle(3) exposures with ~1 electron charge per subaperture per 4 cycle image and one image at a higher signal level (4) but light turned off during extrafocal times.

These images show qualitatively how well the curvature CCD is transferring charge at extremely low light levels and that the signal detected in the image depends only on the integrated signal levels and not on the numbers of images added together to achieve this signal level. This chapter shows that the CCD meets all the requirements needed to be able to be used as a wavefront sensor in a low light level curvature adaptive optics system. With the results of the CCD characterization another simulation run was started to compare the performance of the CCD with avalanche photo diodes traditionally used for curvature wavefront sensing in astronomy. The results of this simulation are presented in the last section of this paper.

6. CCD PERFORMANCE COMPARED TO APDS

With the results from the CCD characterizations, another simulation was started to compare the performance of the CCD with respect to the performance of the avalanche photo diodes for the 60 ñ element ESO MACAO system taking into account the results obtained with the characterization of the CCDs. The properties and simulation parameters are listed in Table 1.

Property	*APD*	*CCD*
Sky background magnitude	*19.0*	*19.0*
Field of view diameter	*2"*	*2"*
Quantum efficiency	*70%*	*80%*
Dark current [electrons/s]	*250*	*0*
Read-out noise [electrons RMS]	*0*	*1.5*
Read-out delay [µs]	*0*	*250*
Seeing [arcsec]	*0.65*	*0.65*

Table 1 Specifications of the curvature wavefront sensor detector for APDs and CCD

Figure 14 shows the results for the CCD. The CCD performs as well as APDs over the entire range of magnitudes down to very faint guide stars at magnitude 18. The plot shows a small difference of the performance of the CCD of 3% at magnitude 15 compared to APDs. At lower light levels the CCD outperforms the APDs due to its higher quantum efficiency. Note that this comparison is only a relative comparison between the detectors and not in terms of absolute Stehl for an AO-system. Different models of the atmosphere and the inner setup of the rest of the AO system like the characteristics of the deformable mirrors would give a different result in overall Strehl. However this does not affect the relative comparison of the wavefront sensors.

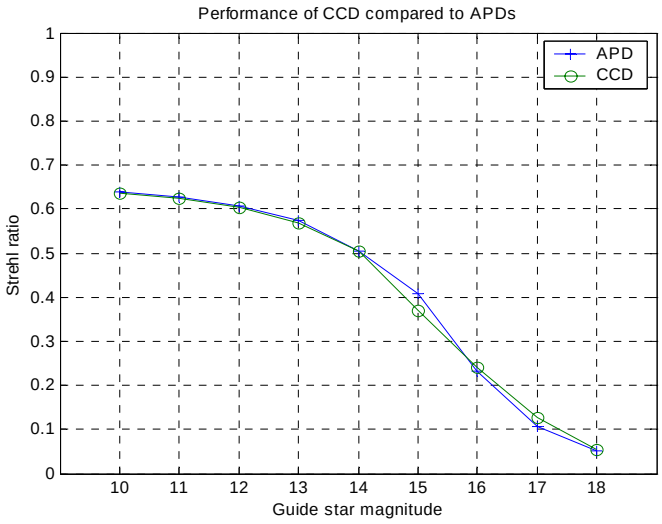

Figure 14 Performance of the curvature CCD with 80% quantum efficiency compared to avalanche photodiodes.

7. CONCLUSIONS

It was demonstrated that the CCD can be operated at noise levels down to 1.5 electrons at a frame rate of 4000 frames per second. This was possible by binning all pixels per subaperture and hence read the serial register at slower speed i.e. 20 µs per superpixel. It was also possible to maintain this noise performance for longer integration times (i.e. integration for more cycles of the membrane) due to the novel design of adding up the charges on the

CCD. Readout noise has been the limiting factor in using standard format CCDs as the wavefront sensor in curvature systems. Furthermore a very demanding requirement for the curvature CCD, the ability to move very small charge packages with high efficiency was demonstrated. This makes the device well suited for low light level applications. The curvature AO CCD is now packaged in backside illuminated versions which are undergoing detailed testing at the moment.
Those detectors will be used by ESO as an upgrade option to the current APD sensors if those have a high failure rate and will be also used by CFHT to upgrade their 19 element PUEO AO system to a 105 element "PUEO NUI" system [6, 7, 8]. This is relatively high order AO for a 3.6-meter telescope, with the goal of producing diffraction-limited images in the red part of the visible spectrum.

ACKNOWLEDGMENTS

The authors would like to thank the members of the many groups at ESO for their constant support and help regarding this project. In particular, Jean Louis Lizon for designing the cryostat and all the mechanical parts needed for the laboratory system; Bernard Delabre, Armin Silber and Christophe Dupuy for all their help with the optical design and the alignment of the relay optics; Siegfried Eschbaumer for soldering the detector board and his help with the setup in the laboratory; Andrea Balestra, Rob Donaldson, Javier Reyes for their support regarding software and hardware related to the FIERA controller. Cyril Cavadore and Boris Gaillard for their help with questions related to PRISM, the software used to reduce most of the data with the curvature CCD. Many thanks also go to Thomas Craven-Bartle, who wrote most of the code for the computer simulations during his masters thesis carried out at ESO and provided also simulation images for the project. We look forward to the on-sky results of the CCID-35 device at CFHT.

REFERENCES

1. Roddier, F. J. and Rigaut, F. (1999), *The UH-CFHT systems* , in Adaptive Optics in Astronomy, ed. Roddier, F. J., Cambridge University Press, Cambridge (UK), 205-34.

2. Donaldson, R., D. Bonaccini, J. Brynnel, B. Buzzoni, L. Close, B. Delabre, C. Dupuy, J. Farinato, E. Fedrigo, N. Hubin, E. Marchetti, S. Stroebele, S Tordo (2000). *MACAO and its application for the VLT interferometer*. In: Adaptive Optical Systems Technology, Munich, Germany, March 27-31, 2000, Proceedings of SPIE, vol. 4007.
3. Beletic, James W., Reinhold J. Dorn, Thomas V. Craven-Bartle, and Barry Burke. *A new CCD designed for curvature wavefront sensing.* Optical Detectors for Astronomy II. Amico, Paola and James W. Beletic, editors. Kluwer Academic Publishers 2000.

4. Craven-Bartle, Thomas V., Reinhold J. Dorn, and James W. Beletic. *Computer simulation comparison of CCDs and APDs for curvature wavefront sensing*. Proceedings of the SPIE Vol. 4007, pp. 444-451, Adaptive Optical Systems Technology. Wizinowich, Peter L., editor. SPIE 2000.

5. Dorn, Reinhold J. *A CCD based curvature wavefront sensor for Adaptive Optics in Astronomy*. Ph.D. thesis. University of Heidelberg, Germany. 2001.

6. Cuillandre, Jean Charles, James W. Beletic, Reinhold J. Dorn, Gerard A. Luppino, Sidik Isani, Nicolas Gorceix, Olivier Lai, Thomas V. Craven-Bartle, Barry Burke and Francois Menard. *FlyEyes: a dual CCD detector system for CFHT PUEO NUI's wavefront sensor*. Proceedings of the SPIE, Vol. 4839, pp. 272-279, Adaptive Optical System Technologies II. Wizinowich, Peter L. and Domenico Bonaccini, editors. SPIE 2002.

7. Lai, Olivier, Francois Menard and Jean-Charles Cuillandre. *PUEO NUI: feasible and fast upgrade of the CFHT adaptive optics system for high-dynamic range imaging.* Proceedings of the SPIE, Volume 4839, pp. 659-672, Adaptive Optical System Technologies II. Wizinowich, Peter L. and Domenico Bonaccini, editors. SPIE 2002.

8. MÈnard, Francois, Olivier Lai and Jean-Charles Cuillandre. *Science with CFHT's future high dynamic range AO system PUEO NUI.* Proceedings of the SPIE, Vol. 4839, pp. 1110-1116, Adaptive Optical System Technologies II. Wizinowich, Peter L. and Domenico Bonaccini, editors. SPIE 2002.